ELSEVIER

Inorganica Chimica Acta 273 (1998) 1–7

Inorganica Chimica Acta

Chelate ring-opening ruthenium complexes: X-ray crystal structure and solution studies of *cis*, *trans*-bis(2-dimethyl-aminoethyl)-diphenyl-phosphino(dichloro)ruthenium(II)

Zijian Guo [a], Abraha Habtemariam [a], Peter J. Sadler [a,*], Brian R. James [b]

[a] *Department of Chemistry, The University of Edinburgh, Edinburgh EH9 3JJ, UK*

[b] *Department of Chemistry, University of British Columbia, Vancouver, BC V6T 1Z1, Canada*

Received 3 April 1997; revised 22 May 1997; accepted 13 June 1997

Abstract

The Ru(II) complex *cis,trans*-[Ru($Me_2NCH_2CH_2PPh_2$-*P,N*)$_2Cl_2$] (**1**) has been characterized in the solid state and in solution. X-ray crystallography showed that complex **1** is monoclinic, space group C_2/c; $a = 36.0421$, $b = 11.4866$, $c = 31.0540$ Å; $\beta = 104.556°$. The structure refined to $R = 0.0925$ and $Rw = 0.223$. There are two independent molecules in the unit cell, with normal Ru–P bonds (2.24–2.26 Å), but the Ru–N bonds (2.37–2.42 Å) are 0.2 Å longer than typical values for Ru–N *trans* to phosphorus. The Cl–Ru–Cl bond angles of **1** are 171.78 and 173.14°. Complex **1** is stable in methylene chloride solution and cyclic voltammetry showed that it undergoes a fully reversible one-electron oxidation at 0.326 V. In methanol, however, **1** (both in air or under N_2) undergoes a two-stage ionization/solvolysis with first order constants at 293 K: $5.40 \pm 0.02 \times 10^{-4}$ s^{-1} for the first step, and $3.29 \pm 0.03 \times 10^{-5}$ s^{-1} for the second step accompanied by a colour change from red to green. ^{1}H and ^{31}P{^{1}H} NMR spectroscopic studies suggest that the solvolysis is accompanied by P,N-chelate ring-opening. These processes are inhibited by the presence of excess of lithium chloride.

Keywords: Ruthenium complexes; Aminophosphine complexes; Crystal structures; Chelate ring complexes

1. Introduction

Several Ru(II) and Ru(III) complexes have been shown to exhibit antitumour activity [1], including *trans*-[$RuCl_2(DMSO)_4$], *trans*-[$RuCl_4$(imidazole)$_2$]$^-$ and *trans*-[$RuCl_4$(indazole)$_2$]$^-$ [2–4]. The most interesting feature of these complexes is their anti-metastatic property which is lacking in platinum-based drugs. The mechanism of action of the Ru(II) complexes is believed to involve binding to DNA [5], but could also involve protein binding. It is believed that Ru(III) complexes are prodrugs which are reduced to Ru(II) prior to DNA binding or inhibition of DNA polymerase [6]. Recent data appear to show that both aquation and reduction of Ru(III) complexes play roles in their activation [7].

We have reported recently that Pt–aminophosphine complexes in aqueous solution exhibit interesting ring-opening and closing equilibria which can be controlled by varying either the pH of the solution or the chloride concentration [8]. These ring-opened Pt(II) complexes can readily bind to the DNA bases guanine and thymine [9]; moreover, they are cytotoxic to cancer cells, e.g. lung carcinoma and OVXF ovarian adenocarcinoma cells, in vitro.

The catalytic properties of ruthenium complexes with different P–N ligand systems (where P and N represent tertiary phosphine and tertiary amine centres, respectively) have been the focus of several studies. In particular, ruthenium complexes with chelating P–N ligands have been shown to form dihydrogen complexes [10–12].

Although some Ru–aminophosphine complexes have been synthesized previously [11,13], there are very few X-ray crystal structures available in the literature. One of our groups [11] has reported the structure of the five-coordinate complex dichloro(*o*-diphenylphosphino-*N,N*-dimethylaniline)-[tris(*p*-tolyl)phosphine]ruthenium(II), while Gao et al. [14] have reported the structure of *trans*-dichloro-*N,N'*-bis[(*o*-(di-phenylphosphino)benzylidene]ethylenediamine-ruthenium(II), where the P,N-ligand is tetradentate. Costella et al. [15] have characterized crystallographically the dimeric complex [Ru_2Cl_2(P–N)$_4$]$^-$, where P–N is 1-(diphenylphosphino)-2-(2-pyridyl)ethane. It was suggested that chlo-

* Corresponding author. Tel.: +44 131 650 4729; fax: +44 131 650 6542; e-mail: P.J.Sadler@ed.ac.uk

PII S0020-1693(97)05911-2

ride dissociation from $[RuCl_2(P\text{–}N)_2]$ gave the five-coordinate cation $[RuCl(P\text{–}N)_2]^+$ which dimerizes to the reported structure.

Here we report the synthesis and X-ray crystal structure of the Ru(II) complex *cis,trans*-$[Ru(Me_2N(CH_2)_2PPh_2)_2Cl_2]$ (**1**). The complex has been characterized by UV, NMR spectroscopy and cyclic voltammetry in methylene dichloride. In methanol solution, complex **1** appears to undergo both chloride dissociation and P,N-chelate ring opening.

2. Experimental

2.1. Chemicals

The methanol used for UV studies was distilled over Mg metal, and all other solvents were obtained from Fisher Chemicals and used as supplied.

Dichloromethane (HPLC grade) used for cyclic voltammetric studies was obtained from Prolabo and stored over potassium hydroxide pellets for 1 week before being refluxed over and distilled from phosphorus pentoxide. $[n\text{-}Bu_4N][BF_4]$ was prepared by neutralizing tetrabutylammonium hydroxide with tetrafluoroboric acid, recrystallized twice from a 1:1 water/methanol mixture and dried at 343 K in vacuo for 48 h prior to use.

$Me_2N(CH_2)_2PPh_2$ was prepared according to the general procedure described previously [16]. $RuCl_3 \cdot 3H_2O$ was supplied by Johnson Matthey Ltd and Colonial Metals Inc. *cis*-$[RuCl_2(DMSO)_4]$ was prepared according to the literature method [17].

2.2. Measurements

Electronic absorption spectra were recorded on Hewlett Packard 8452A and Shimadzu UV-2501 PC spectrophotometers with the slit width adjusted to allow 2 nm resolution, and 1 cm path length cells. ^1H NMR spectra were recorded on Varian XL-300, Bruker DMX-500 and Varian-Inova 600 spectrometers, and were internally referenced to TSP. $^{31}P\{^1H\}$ NMR spectra were recorded on Varian XL-300 and Bruker DMX-500 spectrometers and externally referenced to 30% H_3PO_4. The cyclic voltammetry experiments were carried out in $CH_2Cl_2/[n\text{-}Bu_4N][BF_4]$, with an Autolab PGSTAT20 potentiostat equipped with GPES 4.2 software (Eco Chemie). The working electrode was a platinum microdisc of diameter 0.5 mm and the potential reported in this work is quoted relative to a Ag/AgCl reference electrode via $FeCp_2/FeCp_2^+$ (0.375 V). Bulk electrolysis was achieved in a standard three-compartment H-type cell with platinum basket and mesh working and counter electrodes, respectively; the reference electrode was as before. The molar conductivity was measured at 293 K on a 10^{-3} M methanol solution of **1** with a Model RCM15B1 Surfass Conductivity Bridge.

All the measurements were carried out at 293 K unless otherwise indicated.

2.3. Preparation of *cis,trans*-$[Ru(Me_2NCH_2CH_2PPh_2)_2Cl_2]$ (1)

cis-$[RuCl_2(DMSO)_4]$ (142.6 mg, 0.29 mmol) was dissolved in CH_2Cl_2 (3 ml), giving a yellow solution to which the ligand $Me_2N(CH_2)_2PPh_2$ (151.6 mg, 0.59 mmol) was added. After the mixture was stirred for 5 min at room temperature, the colour of the solution changed to red. After 3 h, diethylether (20 ml) was added to the red solution, and a pink solid precipitated. This was re-dissolved in CH_2Cl_2 and precipitated again by diethylether. The product was dried in vacuo over refluxing ethanol for 24 h (yield 57%). *Anal.* Calc. for $C_{32}H_{40}Cl_2N_2P_2Ru$: C, 55.98; H, 5.87; N, 4.08. Found: C, 55.21; H, 5.77; N, 3.87%. Electronic absorption spectrum in CH_2Cl_2: λ_{max} 508 (log ϵ 2.71); λ 372 (shoulder); in methanol: λ_{max} 506 (log ϵ 2.71); λ 362 (shoulder); ^1H NMR ($CDCl_3$):$N(CH_3)_2$, δ 2.80 (s); methylene protons, δ 2.84 (m) and δ 2.91 (m); phenyl protons, *o*- and *m*-, δ 7.02 (t) and δ 7.14 (t), *p*-, δ 7.21 (t). $^{31}P\{^1H\}$ NMR ($CDCl_3$): δ 56.5.

Crystals of **1** suitable for X-ray crystallographic analysis were grown by slowly evaporating a solution of **1** in CH_2Cl_2/Et_2O.

2.4. X-ray crystallographic analysis

2.4.1. Data collection

A crystal of **1** was attached to a glass fibre and mounted on the Siemens SMART system for data collection at 173 K. An initial set of cell constants was calculated from reflections harvested from three sets of 20 frames. These initial sets of frames were oriented such that orthogonal wedges of reciprocal space were surveyed. This produced orientation matrices determined from 281 reflections from the actual data collection. Hemisphere data collection was used.

2.4.2. Solution and refinement

The crystal data for **1** are listed in Table 1. The space group C_2/c determined for **1** was based on systematic absences and intensity statistics [18]. A successful direct-methods solution was calculated which provided most non-hydrogen atoms from the E-map. Several full-matrix least-squares/difference Fourier cycles were performed which located the remainder of the non-hydrogen atoms. All non-hydrogen atoms were refined with anisotropic displacement parameters. All the hydrogen atoms were placed in ideal positions and refined as riding atoms with relative isotropic displacement parameters ($1.2_{(Uis)}$ host for methylene, methyl and aryl).

There were two independent molecules in the asymmetric unit cell, both of which appeared to have rotational twinning. The rotation appeared to be 180° about the *c* axis. After the rotation, *b* becomes $-b$, and *a* transforms to $-a+(-4/7c)$. The two sets of reciprocal lattices overlap well when *c* is $7n$.

Table 1
Crystal data, data collection, solution and refinement for **1**

Crystal data	
Empirical formula	$C_{32}H_{40}Cl_2N_2P_2Ru$
Crystal habit, colour	Block, red
Crystal size (mm)	0.30×0.30×0.15
Crystal system	monoclinic
Space group	C_2/c
a (Å)	36.0421(6)
b (Å)	11.4866(1)
c (Å)	31.0540(5)
β (°)	104.556(1)
Volume (Å^3)	12443.7(3)
Z	16
Formula weight	686.57
Density (calc.) (Mg m^{-3})	1.466
Absorption coefficient (mm^{-1})	0.803
$F(000)$	5664
Data collection	
Diffractometer	Siemens SMART Platform CCD
Wavelength (Å)	0.71073
Temperature (K)	173(2)
θ Range for data collection (°)	1.17–25.06
Index ranges	$-42 \le h \le 41$, $0 \le k \le 13$, $0 \le l \le 37$
No. reflections collected	30682
No. independent reflections	10921 (R_{int} = 0.0549)
Solution and refinement	
System used	SHELXTL-V5.0
Solution	direct methods
Refinement method	full-matrix least-squares on F^2
Weighting scheme	$w = [\sigma^2(F_o^2) + (AP)^2 + (BP)]^{-1}$, where $P = (F_o^2 + 2FC^2))/3$, $A = 0.0298$, and $B = 692.13$
Absorption correction	SADABS (Sheldrick, 1996)
Max. and min. transmission	1.000 and 0.735
Data/restraints/parameters	10897/0/711
R indices ($I > 2\sigma(I) = 8049$)	$R1 = 0.0925$, $wR2 = 0.2233$
R indices (all data)	$R1 = 0.1229$, $wR2 = 0.2582$
Goodness-of-fit on F^2	1.137
Largest difference peak and hole (e Å^{-3})	3.941 and −2.080

3. Results and discussion

3.1. X-ray crystal structure of 1

Compound **1** crystallized in the space group C_2/c with two independent molecules (**1a** and **1b**) in the unit cell; these are shown in Fig. 1. In these molecules, Ru(II) is situated in a distorted octahedral coordination environment, with two chloride ligands in *trans* positions, and two chelated P–N ligands in *cis* positions. This arrangement seems to be sterically crowded, but is apparently preferred to that in which the two phosphorus atoms are mutually *trans* because of their strong *trans* effects [19]. There are no strong intermolecular interactions involved in the crystal packing. The atomic coordinates are listed in Table 2.

The two five-membered rings formed by the chelation of the ligand to Ru(II) adopt $\delta\delta$ conformations in both molecules. The torsion angles for N–C–C–P were found to be 64.5 and 62.1° for molecule **1a**; and 64.4 and 60.4° for molecule **1b**.

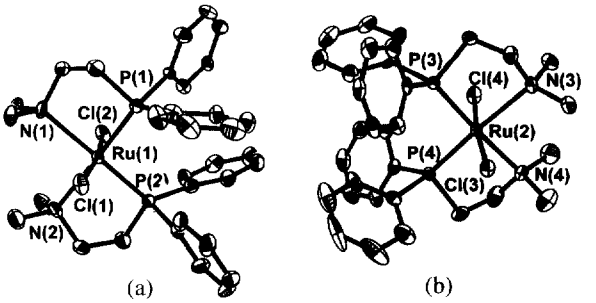

Fig. 1. Crystal structure of *cis,trans*-[Ru($Me_2NCH_2CH_2PPh_2$-*P,N*)$_2Cl_2$] (**1**). The unit cell contains two independent molecules (**1a** and **1b**).

The major bond distances and angles of **1a** and **1b** are listed in Table 3. The Ru–P and Ru–Cl distances are within the range of values typical for Ru(II) complexes [20]. However, the Ru–N bond lengths found in **1a** and **1b**, Ru(1)–N(1), 2.415, Ru(1)–N(2), 2.378, Ru(2)–N(3), 2.403 and Ru(2)–N(4) 2.368 Å are significantly longer (by at least 0.2 Å) than values for *P,N*-chelated Ru(II) complexes reported previously, cf. N *trans* to P in complexes such as *trans*-dichloro-bis(2-diphenylphosphinino)pyridineruthenium(II) (2.13 and 2.06 Å) [21], *trans*-dichloro-*N,N*-bis-[*o*-(diphenylphosphino)benzylidene](ethylenediamine)ruthenium(II) (2.17 and 2.16 Å) [14], and dichlorotetra(1-(diphenylphosphino)-2-(2-pyridyl)ethane)diruthenium(II) (2.152 and 2.157 Å) [15]. The weakening of the Ru–N bonds of complex **1** presumably results from the strong *trans* influence of phosphorus and steric effects due to the methyl substituents on N. The crystal structures of Pt(II) and Pd(II) complexes with the same or similar ligands also show that the M–N bond *trans* to phosphorus is substantially longer than the normal values [22].

The N–Ru–N and P–Ru–P bond angles are in the range 93.9–99.14°, while the orthogonal P–Ru–N angles are smaller, in the range 83.4–83.7°, probably because of strain in the five-membered rings. The less than 180° bond angles for Cl–Ru–Cl (171.78 and 173.14° for **1a** and **1b**, respectively), probably result from steric effects of the phenyl rings. The Cl–Ru–Cl bond angle in *trans*-dichloro-*N,N*-bis-[*o*-(diphenylphosphino)benzylidene]ethylenediamine-ruthenium(II) is as low as 165.4° [14].

3.2. Characterization of cis,trans-[Ru($Me_2NCH_2CH_2PPh_2$)$_2Cl_2$] (1) in solution

Complex **1** is very soluble in chlorinated organic solvents, in acetone and acetonitrile, but insoluble in H_2O. Its solubility in methanol is ~2 mM.

The ^{1}H NMR spectrum of a freshly prepared solution of **1** in $CDCl_3$ exhibited a singlet at 2.80 ppm which can be assigned to the coordinated *N*-methyl protons. The peak is downfield shifted by 0.46 ppm compared with that of the free ligand. The ^{31}P{^{1}H} NMR spectrum of the same solution

Table 2
Atomic coordinates ($\times 10^4$) and equivalent isotropic displacement parameters ($Å^2 \times 10^3$) for **1**

	x	y	z	U_{eq} [a]	SOF
Ru(1)	3767(1)	−975(1)	8167(1)	16(1)	1
Cl(1)	3741(1)	412(2)	8741(1)	29(1)	1
Cl(2)	3793(1)	−2572(2)	7671(1)	27(1)	1
N(1)	3265(3)	−2072(9)	8369(3)	29(2)	1
C(1)	3335(4)	−3354(11)	8406(5)	38(3)	1
C(2)	3175(4)	−1714(14)	8793(4)	44(4)	1
C(3)	2926(3)	−1881(12)	7996(4)	34(3)	1
C(4)	2858(3)	−607(12)	7882(4)	33(3)	1
P(1)	3272(1)	−98(3)	7685(1)	19(1)	1
C(5)	3112(3)	−411(10)	7081(3)	20(2)	1
C(6)	3356(3)	−877(10)	6849(4)	24(2)	1
C(7)	3231(3)	−1041(10)	6392(3)	23(2)	1
C(8)	2872(3)	−722(11)	6161(4)	32(3)	1
C(9)	2626(4)	−210(12)	6396(4)	37(3)	1
C(10)	2746(3)	−60(11)	6847(4)	31(3)	1
C(11)	3218(3)	1494(10)	7663(4)	25(3)	1
C(12)	3116(4)	2132(11)	8001(4)	37(3)	1
C(13)	3111(4)	3350(12)	7994(5)	43(4)	1
C(14)	3193(4)	3928(12)	7642(5)	48(4)	1
C(15)	3280(4)	3330(11)	7298(5)	35(3)	1
C(16)	3293(3)	2104(10)	7309(4)	25(3)	1
N(2)	4272(3)	−1881(8)	8704(3)	25(2)	1
C(17)	4370(4)	−3097(11)	8596(5)	45(4)	1
C(18)	4214(4)	−1935(13)	9166(4)	41(3)	1
C(19)	4611(3)	−1114(12)	8729(4)	35(3)	1
C(20)	4672(3)	−838(13)	8275(4)	36(3)	1
P(2)	4247(1)	−48(3)	7965(1)	19(1)	1
C(21)	4383(3)	1468(12)	8090(4)	30(3)	1
C(22)	4745(4)	1857(13)	8047(4)	41(3)	1
C(23)	4847(5)	3046(15)	8104(5)	55(5)	1
C(24)	4593(5)	3833(14)	8208(5)	50(4)	1
C(25)	4248(5)	3456(12)	8252(4)	44(4)	1
C(26)	4143(4)	2302(11)	8202(4)	31(3)	1
C(27)	4276(3)	−55(10)	7379(4)	26(3)	1
C(28)	4353(4)	−1093(11)	7176(4)	32(3)	1
C(29)	4330(4)	−1119(12)	6723(4)	36(3)	1
C(30)	4227(4)	−134(12)	6469(4)	40(3)	1
C(31)	4148(4)	879(12)	6666(4)	37(3)	1
C(32)	4174(3)	926(12)	7121(4)	33(3)	1
Ru(2)	3786(1)	6015(1)	5131(1)	14(1)	1
Cl(3)	3901(1)	7530(2)	5682(1)	25(1)	1
Cl(4)	3683(1)	4665(2)	4515(1)	27(1)	1
N(3)	3318(3)	7304(8)	4685(3)	22(2)	1
C(33)	3217(3)	7023(12)	4199(3)	29(3)	1
C(34)	3419(4)	8570(10)	4726(4)	34(3)	1
C(35)	2971(3)	7156(10)	4855(4)	26(3)	1
C(36)	2872(3)	5885(11)	4898(4)	25(3)	1
P(3)	3274(1)	5258(2)	5325(1)	18(1)	1
C(37)	3165(3)	3684(10)	5304(4)	23(3)	1
C(38)	3041(4)	3121(11)	4905(4)	33(3)	1
C(39)	2983(4)	1914(12)	4896(5)	38(3)	1
C(40)	3060(4)	1272(13)	5294(5)	47(4)	1
C(41)	3180(4)	1850(11)	5690(5)	40(3)	1
C(42)	3235(3)	3045(10)	5700(4)	29(3)	1
C(43)	3136(3)	5631(9)	5845(3)	19(2)	1
C(44)	2755(3)	5472(11)	5861(4)	28(3)	1
C(45)	2643(4)	5697(12)	6251(4)	34(3)	1
C(46)	2918(4)	6042(10)	6626(4)	28(3)	1
C(47)	3291(4)	6175(10)	6616(4)	31(3)	1
C(48)	3407(3)	5985(10)	6230(4)	25(2)	1
N(4)	4298(3)	6774(8)	4866(3)	23(2)	1
C(49)	4225(4)	6841(14)	4372(4)	45(4)	1
C(50)	4439(4)	7933(13)	5037(5)	49(4)	1
C(51)	4615(4)	5917(12)	5004(4)	39(3)	1
C(52)	4685(3)	5596(11)	5483(4)	30(3)	1
P(4)	4249(1)	4945(2)	5572(1)	19(1)	1
C(53)	4324(3)	4985(10)	6181(4)	22(2)	1
C(54)	4540(4)	5857(12)	6445(5)	42(3)	1
C(55)	4560(5)	5858(15)	6908(5)	63(5)	1
C(56)	4373(6)	5074(16)	7096(5)	69(6)	1
C(57)	4168(5)	4202(15)	6836(5)	54(4)	1
C(58)	4148(3)	4143(12)	6389(4)	34(3)	1
C(59)	4339(3)	3367(10)	5511(4)	22(2)	1
C(60)	4684(4)	2911(10)	5754(4)	30(3)	1
C(61)	4755(4)	1719(12)	5730(5)	41(3)	1
C(62)	4489(4)	1004(12)	5479(5)	41(3)	1
C(63)	4144(4)	1441(12)	5242(4)	39(3)	1
C(64)	4058(3)	2615(9)	5251(4)	24(2)	1

[a] U_{eq} is defined as one third of the trace of the orthogonalized U_{ij} tensor.

Table 3
Selected bond lengths (Å) and angles (°) for **1**

Ru(1)–P(2)	2.249(3)	Ru(1)–P(1)	2.258(3)
Ru(1)–N(2)	2.378(9)	Ru(1)–Cl(2)	2.411(3)
Ru(1)–Cl(1)	2.412(3)	Ru(1)–N(1)	2.415(9)
Ru(2)–P(4)	2.242(3)	Ru(2)–P(3)	2.253(3)
Ru(2)–N(4)	2.368(9)	Ru(2)–N(3)	2.403(9)
Ru(2)–Cl(3)	2.403(3)	Ru(2)–Cl(4)	2.417(3)
P(2)–Ru(1)–P(1)	98.01(10)	P(2)–Ru(1)–N(2)	84.0(2)
P(1)–Ru(1)–N(2)	177.0(2)	P(2)–Ru(1)–Cl(2)	91.49(11)
P(1)–Ru(1)–Cl(2)	93.88(10)	N(2)–Ru(1)–Cl(2)	88.2(2)
P(2)–Ru(1)–Cl(1)	94.02(11)	P(1)–Ru(1)–Cl(1)	91.38(10)
N(2)–Ru(1)–Cl(1)	86.3(2)	Cl(2)–Ru(1)–Cl(1)	171.78(10)
P(2)–Ru(1)–N(1)	176.7(3)	P(1)–Ru(1)–N(1)	83.4(3)
N(2)–Ru(1)–N(1)	94.6(3)	Cl(2)–Ru(1)–N(1)	85.5(3)
Cl(1)–Ru(1)–N(1)	88.9(2)	C(3)–N(1)–C(2)	109.4(10)
P(4)–Ru(2)–N(4)	83.5(2)	P(3)–Ru(2)–N(4)	175.4(2)
P(4)–Ru(2)–N(3)	175.2(2)	P(3)–Ru(2)–N(3)	83.7(2)
P(4)–Ru(2)–P(3)	99.14(10)	N(4)–Ru(2)–N(3)	93.9(3)
P(4)–Ru(2)–Cl(3)	89.57(10)	P(3)–Ru(2)–Cl(3)	95.53(10)
N(4)–Ru(2)–Cl(3)	88.3(2)	N(3)–Ru(2)–Cl(3)	86.3(2)
P(4)–Ru(2)–Cl(4)	94.28(11)	P(3)–Ru(2)–Cl(4)	89.46(10)
N(4)–Ru(2)–Cl(4)	86.5(2)	N(3)–Ru(2)–Cl(4)	89.6(2)
Cl(3)–Ru(2)–Cl(4)	173.14(10)		

showed only a singlet at 56.5 ppm. This chemical shift value corresponds to that expected for a chelated ligand, as observed for analogous Pd and Pt complexes [23].

Cyclic voltammetry of **1** revealed a reversible oxidation at 0.326 V (versus Ag/AgCl) in CH_2Cl_2 (Fig. 2). A plot of peak height against the square root of the scan rate confirmed that the process was diffusion controlled. This redox process can be assigned to the metal-centred Ru(II)–Ru(III) couple. While the compound showed no reductive electrochemistry within the accessible potential window, a multielectron irreversible oxidation process was observed, which may be

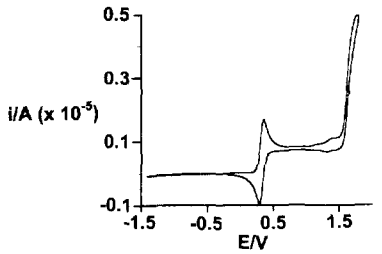

Fig. 2. Cyclic voltammogram of *cis,trans*-[Ru($Me_2NCH_2CH_2PPh_2$-*P,N*)$_2$-Cl_2] (**1**) in 0.4 M [n-Bu_4N][BF_4]/CH_2Cl_2 at 293 K. A fully reversible one-electron redox process is observed at 0.326 V.

related to the further oxidation of ruthenium or to the oxidation of the phosphine to phosphine oxide. The value of the redox couple can be compared with the value predicted by the ligand additivity model proposed by Lever [24]. On the basis of two chlorides, two N atoms as butylamines and two P atoms as methyldiphenylphosphines (from the available tabulated data), a value of 0.25 V was calculated, which on addition of 0.05 V as solvent correction [25] gives a calculated value of 0.30 V, close to the observed value.

The oxidation of complex **1** was effected by bulk electrolysis at 0.75 V. Coulometry confirmed that the redox process is a one-electron oxidation. This produced a solution with a much more intense red colour, and a UV spectrum of which contained three bands at 343, 421 and 528 nm. The oxidized compound is likely to be the cationic Ru(III) analogue of complex **1**.

3.3. Solution behaviour of *1* in methanol

While compound **1** is stable in CH_2Cl_2, it undergoes a series of reactions in MeOH accompanied by colour changes, either in air or under N_2 or Ar.

A fresh solution of **1** in d_4-MeOD was monitored by ^1H and $^{31}P\{^1H\}$ NMR. In the ^1H NMR spectrum, the signals assignable to **1** have similar shifts to those observed in $CDCl_3$. However, all the signals were somewhat broader than for the $CDCl_3$ solution and without clearly resolved couplings. The spectrum recorded after 20 min showed the appearance of new signals in the aromatic and methyl regions. In the aromatic region, new low field signals appeared. These new signals never became the major species in the spectrum during the period studied. After 1 h, another set of new signals appeared at 7.68(m), 7.72(m), 7.86(m) ppm which steadily increased in intensity and eventually became the predominant ones after 7 h. In the meantime, in the methyl region of the spectrum, a major new singlet appeared at 2.64 ppm which has a shift comparable with that of a free (unbound) $-N(CH_3)_2$ group. This suggested that ring-opening had occurred, leading to coordination of the ligand through phosphorus only.

The $^{31}P\{^1H\}$ NMR spectrum of complex **1** in d_4-MeOD initially contained a singlet peak at 56.0 ppm. After 1 h, a new singlet appeared at 54.1 ppm, i.e. at the same time as new peaks were observed in the ^1H NMR spectrum. Similarly, this signal never became the predominant species. After 4 h, a new signal appeared at 34.2 ppm which steadily increased in intensity until it dominated the spectrum after 8 h. The chemical shift of the peak is similar to that for the aminophosphine ligand bound (to Pt(II)) [8] via P only. Thus **1** reacts with methanol to give a mixture of complexes, amongst which is a ring-opened complex with two pendant $-N(CH_3)_2$ arms.

The UV spectrum of **1** in methanol under N_2 undergoes two sets of changes with time (Fig. 3). During the first hour (Fig. 3(a)) the absorption at 506 nm decreased with time, while a shoulder at 366 nm increased in intensity and appeared as a band after 20 min. An isosbestic point was observed at 480 nm, and the colour of the solution changed from red to pale orange. After a further 1 h, the colour of the solution gradually turned to green. A new broad band at 621 nm appeared and increased in intensity with time (Fig. 3(b)), while the intensity of the 366 nm band increased throughout the first 13 h. This second set of spectral changes gave rise to another isosbestic point at 518 nm. By following the intensity decrease at λ_{506} with time for the first step, and using Guggenheim treatment [26], a first order rate constant of $5.40 \pm 0.02 \times 10^{-4}\ s^{-1}$ ($t_{1/2} = 20$ min) was obtained at 293 K. Similarly, for the second step, by following the intensity increase at λ_{621} and using the same method, a first order rate constant of $3.29 \pm 0.03 \times 10^{-5}\ s^{-1}$ ($t_{1/2} = 5.85$ h) was obtained. The green solution obtained after 2 days was stable (no further changes in the absorption spectrum). The conductivity of the solution at that time was determined to be

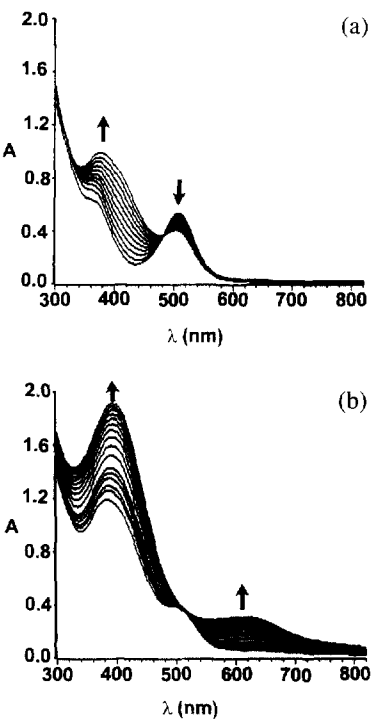

Fig. 3. Electronic absorption spectra of *cis,trans*-[Ru($Me_2NCH_2CH_2PPh_2$-*P,N*)$_2$$Cl_2$] (**1**) ($1.0 \times 10^{-3}$ M) recorded at 293 K in MeOH under N_2. (a) Spectra recorded during the first 55 min after dissolution, at time intervals of 5 min. (b) Spectra recorded between 2 and 13 h.

104 Ω^{-1} cm^2 mol^{-1}, which is in the region expected for 1:1 electrolyte [27].

Solutions of complex **1** in methanol in the presence of 0.1 M LiCl were also monitored at 293 K by ^{1}H and ^{31}P{^{1}H} NMR (2 mM, d_4-MeOD) and by electronic absorption spectroscopy (1 mM, MeOH). In the ^{1}H and ^{31}P{^{1}H} NMR spectra, no new signals were observed even after 10 h. In the visible absorption spectrum, the decrease in intensity of the 506 nm band and the increase in intensity of 375 nm band occurred only very slowly, and the broad band at 620 nm began to appear only after 20 h.

Taken together, the ^{1}H NMR and electronic spectroscopic data suggest that **1** undergoes a two-step reaction in methanol which involves chloride dissociation followed by P,N-chelate ring-opening of **1**. Chloride inhibits the solvolysis process, and chloride release appears to be necessary for the chelate ring-opening reaction.

It has been reported that *trans*-dichlorobis(1-(diphenylphosphino)-2-(2-pyridyl)ethane-ruthenium(II) in acetonitrile gives a conducting solution, and this was suggested to involve the formation of solvated species such as [RuCl(solvent)(P–N)$_2$]$^+$ [15]. It was also suggested that the same precursor can isomerize to the *cis* analogue in CH_2Cl_2, followed by the dissociation of chloride to give the five-coordinate cation [RuCl(P–N)$_2$]$^+$.

As discussed in Section 3.1, complex **1** has rather long and weak Ru–N bonds. This may facilitate the P,N-chelate ring-opening by a coordinating solvent such as methanol. We have found [8,22] that analogous palladium and platinum complexes with the same or similar ligands can readily form ring-opened complexes.

4. Conclusions

The ruthenium complex *cis,trans*-[Ru(Me$_2$NCH$_2$CH$_2$-PPh$_2$)$_2$Cl$_2$] (**1**) has been prepared and shown to have unusually long Ru–N bonds. In methanol solution, the complex undergoes a two-step reaction which appears to involve solvolysis followed by chelate ring-opening. These processes are inhibited by the presence of excess of chloride; such control of chelate ring-opening may lead to potentially interesting biological properties. Electrochemical studies show that oxidation of **1** can readily be achieved, giving the Ru(III) analogue, a complex which may be of interest for anticancer (antimetastatic) studies.

5. Supplementary material

Hydrogen atom coordinates, thermal parameters, tables of observed and calculated structure factors are available from the corresponding author on request.

Acknowledgements

We thank the Association for International Cancer Research, BBSRC, EPSRC, EC COST Action D1, and NSERC of Canada for their support for this work, and Johnson Matthey plc. and Colonial Metals Inc. for the loan of ruthenium. We thank Drs L.J. Yellowlees, K.J. Taylor and A.R. Brown (University of Edinburgh) for the electrochemical measurements and helpful discussion, Dr J.A. Parkinson (University of Edinburgh) for recording some of the NMR spectra, Mr P. Borda (University of British Columbia) for the elemental analysis, and Dr Victor G. Young, Jr of the X-ray Crystallographic Laboratory, University of Minnesota, for determination of the crystal structure. We also thank Professor K. Kirchner for informing us (personal communication) that his group has recently synthesized complex **1** by a different route, and determined the structure of its acetone/chloroform solvate.

References

[1] (a) B.K. Keppler, New J. Chem., 14 (1990) 389; (b) M.J. Clarke, V.M. Bailey, P.E. Doan, C.D. Hiller, K.J. LaChance-Galang, H. Daghlian, S.Mandal, C.M. Bastos and D. Lang, Inorg. Chem., 35 (1996) 4896.

[2] (a) E. Alessio, G. Mestroni, G. Nardin, W.M. Attia, M. Calligaris, G. Sava and S. Zorzet, Inorg. Chem., 27 (1988) 4099; (b) G. Mestroni, E. Alessio, G. Sava, S. Pacor, M. Coluccia and A. Boccarelli, Metal-Based Drugs, 1 (1994) 41.

[3] B.K. Keppler, M. Henn, U.M. Juhl, M.R. Berger, R. Niebl and F.E. Wagner, Prog. Clin. Biochem. Med., 10 (1989) 41.

[4] F. Kratz, B.K. Keppler, M. Hartmann, L. Messori and M.R. Berger, Metal-Based Drugs, 3 (1996) 15.

[5] (a) G. Mestroni, E. Alessio, G. Sava, S. Pacor and M. Coluccia, in B.K. Keppler (ed.), Metal Complexes in Cancer Chemotherapy, VCH, Weinheim, Germany, 1993, p. 157; (b) F. Loseto, E. Alessio, G. Mestroni, G. Lacidogna, A. Nassi, D. Giordano and M. Coluccia, Anticancer Res., 11 (1991) 1549.

[6] A. Galeano, M.R. Berger and B.K. Keppler, Arzneim. Forsch. Drug Res., 42 (1992) 821.

[7] O.M. Ni. Dhubhghaill, W.R. Hagen, B.K. Keppler, K.-G. Lipponer and P.J. Sadler, J. Chem. Soc., Dalton Trans., (1994) 3305.

[8] A. Habtemariam and P.J. Sadler, J. Chem. Soc., Chem. Commun., (1996) 1785.

[9] N. Margiotta, A. Habtemariam and P.J. Sadler, Angew. Chem., Int. Ed., 36 (1997) 1185.

[10] (a) C. Hampton, W.R. Cullen, B.R. James and J.-P. Charland, J. Am. Chem. Soc., 110 (1988) 6918; (b) C.R.S.M. Hampton, I.R. Butler, W.R. Cullen, B.R. James, J.-P. Charland and J. Simpson, Inorg. Chem., 31 (1992) 5509.

[11] C. Mudalige, S.J. Rettig, W.R. Cullen and B.R. James, J. Chem. Soc., Chem. Commun. (1993) 830.

[12] A.A. Batista, E.A. Polato, S.L. Queiroz, O.R. Nascimento, B.R. James and S.J. Rettig, Inorg. Chim. Acta, 230 (1995) 111.

[13] M.M.T. Khan and A.P. Reddy, Polyhedron, 6 (1987) 2009.

[14] J.-X. Gao, H.-L. Wan, W.-K. Wong, M.-C. Tse and W.-T. Wong, Polyhedron, 15 (1996) 1241.

[15] L. Costella, A. Del Zotto, A. Mezzetti, E. Zangrando and P. Rigo, J. Chem. Soc., Dalton Trans., (1993) 3001.

[16] T. Hayashi, M. Konishi, M. Fukushima, K. Kanehira, T. Hioki and M. Kumada, J. Org. Chem., 48 (1983) 2195.

[17] (a) A.M. Joshi, Ph.D. Dissertation, The University of British Columbia, Vancouver, Canada, 1990; (b) I.P. Evans, A. Spencer and G. Wilkinson, J. Chem. Soc., Dalton Trans., (1973) 204.
[18] SHELXTL-plus V5.0, Siemens Industrial Automation Inc., Madison, WI.
[19] F.A. Cotton and G. Wilkinson, Advanced Inorganic Chemistry, Wiley, New York, 4th edn., 1980, p. 1200.
[20] A.G. Orpen, L. Brammer, F.H. Allen, O. Kennard, D.G. Watson and R. Taylor, J. Chem. Soc., Dalton Trans., (1989) S1, 83; A.M. Joshi, I.S. Thorburn, S.J. Rettig and B.R. James, Inorg. Chim. Acta, 198–200 (1992) 283.
[21] D. Drommi, F. Nicolo, C.G. Arena, G. Bruno, F. Faraone and R. Gobetto, Inorg. Chim. Acta, 221 (1994) 109.
[22] A. Habtemariam, R. Palmer, B. Potter and P.J. Sadler, manuscript in preparation.
[23] P.E. Garrou, Chem. Rev., 81 (1981) 229.
[24] A.B.P. Lever, Inorg. Chem., 29 (1990) 1271.
[25] K.J. Taylor, personal communication, 1997.
[26] D.P. Shoemaker and C.W. Garland, Experiments in Physical Chemistry, McGraw-Hill, New York, 1962, p. 222.
[27] W.J. Geary, Coord. Chem. Rev., 7 (1971) 81.